

Dynamic Real-time Optimization of Batch Processes using Pontryagin's Minimum Principle and Set-membership Adaptation

Radoslav Paulen^{a,1}, Miroslav Fikar^a

^a*Faculty of Chemical and Food Technology, Slovak University of Technology in
Bratislava, Radlinskeho 9, Bratislava, Slovakia*

Abstract

This paper studies a dynamic real-time optimization in the context of model-based time-optimal operation of batch processes under parametric model mismatch. In order to tackle the model-mismatch issue, a receding-horizon policy is usually followed with frequent re-optimization. The main problem addressed in this study is the high computational burden that is usually required by such schemes. We propose an approach that uses parameterized conditions of optimality in the adaptive predictive-control fashion. The uncertainty in the model predictions is treated explicitly using reachable sets that are projected into the optimality conditions. Adaptation of model parameters is performed online using set-membership estimation. A class of batch membrane separation processes is in the scope of the presented applications, where the benefits of the presented approach are outlined.

Keywords: dynamic real-time optimization, batch processes, membrane separation, set-membership estimation

*Corresponding author. Tel.: +421 259 325 730; fax: +421 259 325 340.
Email address: radoslav.paulen@stuba.sk (Radoslav Paulen)

1. Introduction

Optimization of operations of batch processes is a rich field of research. One of the main goals is to reduce the variability among the produced batches despite the present uncertainties and disturbances. This problem struck the attention of many research groups (Nagy and Braatz, 2003; Srinivasan et al., 2003a; Adetola et al., 2009; François and Bonvin, 2013; Lucia et al., 2013; Martí et al., 2015; Jang et al., 2016).

In this paper, we consider a real-time implementation of a control policy under parametric plant-model mismatch that optimizes a batch process by assigning dynamic degrees of freedom such that a certain performance index is optimized. Similar problems were studied in many previous works using on-line or batch-to-batch adaptation of the optimality conditions (François et al., 2005; François and Bonvin, 2013), by mid-course correction (Yabuki and MacGregor, 1997; Hosseini et al., 2013) or by design of robust controller for tracking the conditions of optimality (Nagy and Braatz, 2003). Another set of approaches to the problem uses advanced robust strategies in the framework of model predictive control (Lucia et al., 2013). This paper proposes an adaptation of these approaches to the problem of dynamic real-time optimization of batch processes. This task is not straightforward because if one uses a receding-horizon control strategy, the prediction horizons used need to be quite long, because of the usual presence of terminal constraints, which might compromise the real-time feasibility of the scheme.

We base the presented methodology on the parameterization of the optimal operation using the optimality conditions given by Pontryagin's min-

imum principle. As the cost is usually insensitive w.r.t. a precise singular control trajectory (Srinivasan et al., 2003a), the parameterization of the optimal policy makes the real-time decision problem to mainly boil down to identification of switching times of the optimal control policy. Such approach reduces computational burden while allowing for the use of sufficiently long prediction horizons when projecting the parametric uncertainty in controller performance and feasibility, particularly w.r.t. terminal time conditions. Robustness w.r.t. parametric uncertainty is addressed by taking into account the imprecision of parameter estimates, which is projected into the uncertainty of the switching times. In order to improve performance of such a controller, i.e., to reduce conservatism introduced by uncertain switching times, we use on-line parameter estimation. While having the optimal control policy explicitly parameterized in the uncertain parameters, one can tailor the real-time implementation of the optimal operation, e.g., in a way that minimizes the number of on-line calculations.

The novelty of this paper lies foremost in an effective combination of Pontryagin's minimum principle and set-based techniques (set-membership estimation and reachability analysis). This gives rise to a methodology capable of projecting the propagation of the uncertainty in model parameters into uncertainty in the optimal operation of a plant. Using this methodology, efficient and effective real-time optimization of a plant can be established.

The outline of the paper is as follows. Section 3 present preliminary theoretical knowledge on Pontryagin's minimum principle (Pontryagin et al., 1962) and on set-membership estimation (Schweppe, 1968; Fogel and Huang, 1982). The former is used to parameterize the optimality conditions of the

dynamic optimization problem, while the latter technique is used for adaptation of the model parameters based on the measured data along the process run. Next we propose the implementation of the real-time optimization using parameter adaptation. Finally, we present a case study from chemical engineering domain and discuss various aspects of the obtained results.

2. Problem definition

In this paper, we consider a real-time implementation of a control policy that optimizes a process by assigning dynamic degrees of freedom such that a certain performance index is optimized:

$$\min_{u(t), t_f} \mathcal{J}(\mathbf{p}) := \min_{u(t), t_f} \int_0^{t_f} F_0(\mathbf{x}(t, \mathbf{p}), \mathbf{p}) + F_u(\mathbf{x}(t, \mathbf{p}), \mathbf{p})u(t) dt \quad (1a)$$

$$\text{s.t. } \dot{\mathbf{x}}(t, \mathbf{p}) = \mathbf{f}_0(\mathbf{x}(t, \mathbf{p}), \mathbf{p}) + \mathbf{f}_u(\mathbf{x}(t, \mathbf{p}), \mathbf{p})u(t), \quad (1b)$$

$$\mathbf{x}(0) = \mathbf{x}_0, \quad \mathbf{x}(t_f, \mathbf{p}) = \mathbf{x}_f, \quad (1c)$$

$$u(t) \in [u^L, u^U], \quad (1d)$$

where t is time with $t \in [0, t_f]$, $\mathbf{x}(\cdot)$ is an n -dimensional vector of state variables, \mathbf{p} is an m -dimensional vector of model parameters, $u(t)$ is a (scalar) manipulated variable, $F_0(\cdot)$, $F_u(\cdot)$, $\mathbf{f}_0(\cdot)$, and $\mathbf{f}_u(\cdot)$ are continuously differentiable functions, \mathbf{x}_0 represents a vector of initial conditions, and \mathbf{x}_f are specified final conditions. We note here that an inclusion of multi-input and/or state-constrained cases is a straightforward extension but it is not considered in this study for the sake of simplicity of the presentation. We also note that the specific class of input-affine systems is a suitable representation for a large variety of the controlled systems (Hangos et al., 2006). For a general nonlinear model, one may use simple manipulations to rearrange the model

into input-affine structure (Sontag, 1998), which might though increase the number states of the problem. In the domain of chemical engineering, it is, however, very common to encounter input-affine problems (Amrhein et al., 2010) (e.g., when the optimized variable is a reactor feed) or to reformulate the model and arrive at the input-affine structure (Liou and Hsiue, 1995).

We will assume that the plant behavior is known qualitatively and that the only source of uncertainty is present in the unknown values of model parameters. Only a prior knowledge is assumed about the parameters, i.e., the true values of the parameters lie in the a priori known interval box $\mathbf{P}_0 := [\mathbf{p}_0^L, \mathbf{p}_0^U]$, where superscripts L and U denote the lower and upper bounds of \mathbf{p} . The nominal realization of the uncertainty will be assumed as $\mathbf{p}^{\text{nom}} := \text{mid}(\mathbf{P})$, where $\text{mid}(\cdot)$ indicates a mid-point of the interval box.

We will also assume that certain measurements are available from the plant. Their corresponding model-based predictions are

$$\mathbf{y}(t) = \mathbf{g}(\mathbf{x}(t, \mathbf{p}), \mathbf{p}), \quad (2)$$

where $\mathbf{g}(\cdot)$ is a continuously differentiable vector function.

3. Preliminaries

3.1. Conditions for Optimality

Pontryagin’s minimum principle can be used (Johnson and Gibson, 1963; Srinivasan et al., 2003b; Paulen et al., 2012, 2015) to identify the optimal solution to (1) via enforcing the necessary conditions for minimization of a

Hamiltonian

$$H := \mu^L(u^L - u) + \mu^U(u - u^U) + \underbrace{F_0 + \boldsymbol{\lambda}^T \mathbf{f}_0}_{H_0(\mathbf{x}(t, \mathbf{p}), \boldsymbol{\lambda}(t, \mathbf{p}), \mathbf{p})} + \underbrace{(F_u + \boldsymbol{\lambda}^T \mathbf{f}_u)}_{H_u(\mathbf{x}(t, \mathbf{p}), \boldsymbol{\lambda}(t, \mathbf{p}), \mathbf{p})} u, \quad (3)$$

where $\boldsymbol{\lambda}(\cdot)$ is a vector of adjoint variables, which are defined through

$$\dot{\boldsymbol{\lambda}}(t, \mathbf{p}) = -\frac{\partial H}{\partial \mathbf{x}}(t, \mathbf{p}), \quad \boldsymbol{\lambda}(t_f, \mathbf{p}) = \boldsymbol{\nu}(\mathbf{p}), \quad (4)$$

and $\mu^L(t, \mathbf{p})$, $\mu^U(t, \mathbf{p})$, and $\boldsymbol{\nu}(\mathbf{p})$ are the corresponding Lagrange multipliers. The optimality conditions of (1) can then be stated as (Srinivasan et al., 2003b): $\forall t \in [0, t_f]$,

$$\frac{\partial H}{\partial u} := H_u(\mathbf{x}(t, \mathbf{p}), \boldsymbol{\lambda}(t, \mathbf{p}), \mathbf{p}) - \mu^L(t, \mathbf{p}) + \mu^U(t, \mathbf{p}) = 0, \quad (5)$$

$$H(\mathbf{x}(t, \mathbf{p}), \boldsymbol{\lambda}(t, \mathbf{p}), \mathbf{p}, u(t), \mu^L(t, \mathbf{p}), \mu^U(t, \mathbf{p})) = 0, \quad (6)$$

$$H_0(\mathbf{x}(t, \mathbf{p}), \boldsymbol{\lambda}(t, \mathbf{p}), \mathbf{p}) = 0, \quad \mathbf{x}(t_f, \mathbf{p}) - \mathbf{x}_f = 0. \quad (7)$$

The condition $H = 0$ arises from the transversality, since the final time is free (Pontryagin et al., 1962), and from the fact that the optimal Hamiltonian is constant over the whole time horizon, as it is not an explicit function of time. The condition $H_0 = 0$ is the consequence of the former two conditions. Since the Hamiltonian is affine in input (see (3)), the optimal trajectory of control variable is either determined by active input constraints or it evolves inside the feasible region.

Assume that for some point t we have $H_u = 0$ and $u^L < u(t) < u^U$. It follows from (5) that the optimal control maintains $H_u(\cdot) = 0$. Such control is traditionally denoted as singular. Further properties of the singular arc, such as switching conditions or state-feedback control trajectory can be obtained by differentiation of H_u with respect to time (sufficiently many

times) and by requiring the derivatives to be zero. The time derivatives of H and H_0 must be equal to zero as well. Earlier results on derivation of optimal control for input-affine systems (Srinivasan et al., 2003b) suggest that it is possible to eliminate $\boldsymbol{\lambda}(\cdot)$ from the optimality conditions and thus to arrive at analytical characterization of switching conditions between singular and saturated-control arcs.

As the optimality conditions obtained by the differentiation w.r.t. time are linear in the adjoint variables, the differentiation of H_u (or H_0) can be carried out until it is possible to transform the obtained conditions to a pure state-dependent switching function $S(\mathbf{x}(t), \mathbf{p})$. It is usually convenient to use a determinant of the coefficient matrix of the equation system $\mathbf{A}\boldsymbol{\lambda} = \mathbf{0}$ for this. The singular control $u_s(\mathbf{x}(t), \mathbf{p})$ can be found from differentiation of switching function w.r.t. time as

$$\begin{aligned} \frac{dS}{dt} &= \frac{\partial S}{\partial \mathbf{x}^T} \frac{d\mathbf{x}}{dt} = \frac{\partial S}{\partial \mathbf{x}^T} (\mathbf{f}_0 + \mathbf{f}_u u_s) = 0 \\ \Rightarrow \quad u_s(\mathbf{x}(t), \mathbf{p}) &= - \frac{\partial S}{\partial \mathbf{x}^T} \mathbf{f}_0 \bigg/ \frac{\partial S}{\partial \mathbf{x}^T} \mathbf{f}_u. \end{aligned} \quad (8)$$

The resulting optimal-control policy is then given as a step-wise strat-

egy (Paulen et al., 2015) by

$$u^*(t, \boldsymbol{\pi}) := \begin{cases} u^L, & t \in [0, t_1), S(\mathbf{x}(t, \mathbf{p}), \mathbf{p}) > 0, \\ u^U, & t \in [0, t_1), S(\mathbf{x}(t, \mathbf{p}), \mathbf{p}) < 0, \\ u_s(\mathbf{x}(t, \mathbf{p}), \mathbf{p}), & t \in [t_1, t_2), S(\mathbf{x}(t, \mathbf{p}), \mathbf{p}) = 0, \\ u^L, & t \in [t_2, t_f], S(\mathbf{x}_f, \mathbf{p}) < 0, \\ u^U, & t \in [t_2, t_f], S(\mathbf{x}_f, \mathbf{p}) > 0, \end{cases} \quad (9)$$

$$\mathbf{x}_f = \mathbf{x}(t_2, \mathbf{p}) + \int_{t_2}^{t_f} \mathbf{f}_0(\mathbf{x}(t, \mathbf{p}), \mathbf{p}) + \mathbf{f}_u(\mathbf{x}(t, \mathbf{p}), \mathbf{p})u^*(t, \boldsymbol{\pi}) dt, \quad (10)$$

where $\boldsymbol{\pi} := (\mathbf{p}^T, t_1, t_2, t_f)^T$ is the vector that parameterizes the optimal control strategy. Note that the presented optimal-control strategy determines implicitly the switching times t_1 , t_2 and the terminal time t_f as functions of model parameters \mathbf{p} .

In case that the use of the minimum principle turns out to be too complex (e.g., many derivatives are needed to characterize the solution), a numerical identification of the control arcs (Schlegel et al., 2005; Schlegel and Marquardt, 2006) or a recently presented parsimonious input parameterization (Aydin et al., 2018; Rodrigues and Bonvin, 2019) can be used.

3.2. Set-membership estimation

In order to estimate the model parameters, we will make use of plant outputs (measurements), whose predictions are expressed as in (2). We will assume that the true output of the plant $\mathbf{y}_p(t)$ is corrupted with a (sensor) noise that is bounded with a known magnitude $\boldsymbol{\sigma}$. Thus, the measured output $\mathbf{y}_m(t)$ is such that

$$|\mathbf{y}_m(t) - \mathbf{y}_p(t)| \leq \boldsymbol{\sigma}, \quad (11)$$

where the absolute value is understood component-wise. In turn, the set-membership constraints for predicted output $\mathbf{y}(t)$ apply in the form:

$$|\mathbf{y}_m(t) - \mathbf{y}(t)| \leq \boldsymbol{\sigma}. \quad (12)$$

We are interested in the determination of parametric bounds such that

$$\mathbf{P}_k \subseteq \mathbf{P}_{k-1} \subseteq \cdots \subseteq \mathbf{P}_1 \subseteq \mathbf{P}_0, \quad (13)$$

where k is the ordinal number of a measurement taken. The parametric bounds can be determined through solution of a series of optimization problems as (Gottu Mukkula and Paulen, 2017; Walz et al., 2018):

$$p_{k,j}^L/p_{k,j}^U := \min_{\mathbf{p} \in \mathbf{P}_0} / \max_{\mathbf{p} \in \mathbf{P}_0} p_j \quad (14a)$$

$$\text{s.t. } \dot{\mathbf{x}}(t, \mathbf{p}) = \mathbf{f}_0(\mathbf{x}(t, \mathbf{p}), \mathbf{p}) + \mathbf{f}_u(\mathbf{x}(t, \mathbf{p}), \mathbf{p})u(t), \quad \forall t \in [0, t_k], \quad (14b)$$

$$\mathbf{x}(0, \mathbf{p}) = \mathbf{h}(\mathbf{p}), \quad (14c)$$

$$\mathbf{y}(t_i, \mathbf{p}) = \mathbf{g}(\mathbf{x}(t_i, \mathbf{p}), \mathbf{p}), \quad \forall i \in \{1, \dots, k\}, \quad (14d)$$

$$-\boldsymbol{\sigma} \leq \mathbf{y}(t_i, \mathbf{p}) - \mathbf{y}_m(t_i) \leq \boldsymbol{\sigma}, \quad \forall i \in \{1, \dots, k\}, \quad (14e)$$

for given $u(t)$, where $j \in \{1, \dots, n_p\}$ indicates the j^{th} element of a vector.

4. Dynamic real-time optimization

As the optimal control structure is a function of uncertain parameters, the uncertainty should be taken into account when devising a real-time implementation of the optimal control of the plant.

4.1. Projection of parametric uncertainty into solution strategy

Given the structure of the optimal-control policy (9), one can project the parametric uncertainty into uncertainty of the switching times and singular

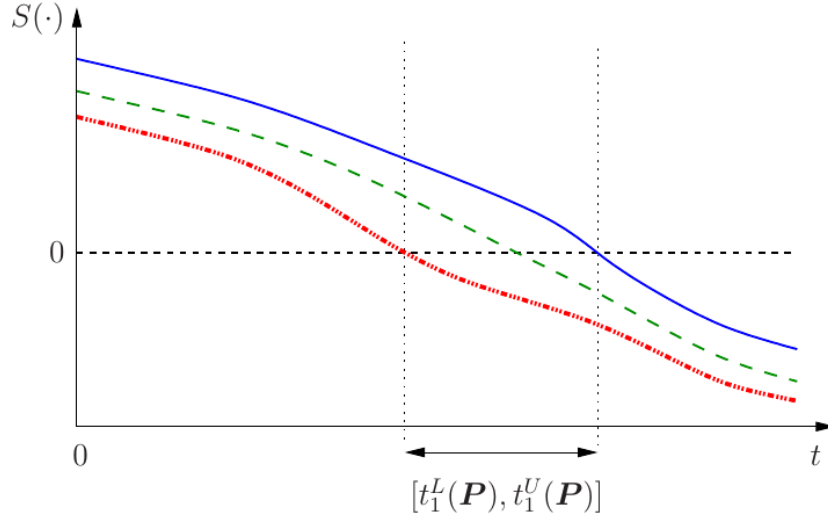


Figure 1: Illustration of the switching function evolution under uncertainty using (set-based) reachability analysis with nominal uncertainty realization (green dashed line) and extreme realizations (dash-dotted red and solid blue lines).

control as $(\forall \mathbf{p} \in \mathbf{P})$

$$t_l(\mathbf{p}) \in [t_l^L(\mathbf{P}), t_l^U(\mathbf{P})] =: T_l, \quad \forall l \in \{1, 2, f\}, \quad (15a)$$

$$u_s(t, \mathbf{p}) \in [u_s^L(t, \mathbf{P}), u_s^U(t, \mathbf{P})] =: U^{\text{opt}}(t), \quad \forall t \in [t_1(\mathbf{p}), t_2(\mathbf{p})]. \quad (15b)$$

This can be achieved either by using some set-theoretic techniques for calculating reachable sets (Chachuat et al., 2015) or by sampling approaches. Figure 1 provides an illustration, where the reachable sets are shown over time for the switching function $S(\cdot)$.

Formally, the problem of determination of (15) can be cast as a set-inversion problem (Jaulin and Walter, 1993). As an example, let us consider

that $S(\mathbf{x}(0, \mathbf{p}), \mathbf{p}) > 0, \forall \mathbf{p} \in \mathbf{P}_0$. The interval T_1 can then be defined as:

$$T_1 := \left\{ t_1 \left| \begin{array}{l} \exists \mathbf{p} \in \mathbf{P}, \forall t \in [0, t_1] : \\ \mathbf{x}(0, \mathbf{p}) = \mathbf{h}(\mathbf{p}), S(\mathbf{x}(t_1, \mathbf{p}), \mathbf{p}) = 0, \\ \dot{\mathbf{x}}(t, \mathbf{p}) = \mathbf{f}_0(\mathbf{x}(t, \mathbf{p}), \mathbf{p}) + \mathbf{f}_u(\mathbf{x}(t, \mathbf{p}), \mathbf{p})u^L \end{array} \right. \right\}. \quad (16)$$

The rest of the uncertain intervals and controls can be defined and determined analogously. Efficient set-inversion techniques exist (Paulen et al., 2016) and can be used herein. The problem might also be reformulated to a bound-determining optimization problem, similarly to the estimation problem in (14). Using such a reformulation, it is also possible to merge the problems of reachability analysis and set-membership estimation and to formulate the reachability-analysis problem directly over the collected data. This way several possible deficiencies (such as those arising from outbounding the parameter set by a box) can be eliminated.

Figure 2 illustrates the parameterization (15) for a simple case, where the singular control is constant. Note that the parameterization reveals time intervals (i.e., $[0, t_1^L(\mathbf{P})]$, $[t_1^U(\mathbf{P}), t_2^L(\mathbf{P})]$, and $[t_2^U(\mathbf{P}), t_f^L(\mathbf{P})]$), which are parts of the optimal solution for any realization of uncertain parameters and are thus invariant to the presence of uncertainty.

A particular technical advantage can be exploited for determination of the switching intervals i.e., that the integration in (10) can be done backwards in time from the final condition. As the batch processes exhibit inherently unstable dynamics, their backward integration is stable (Cao et al., 2003). Such a feature can readily be exploited by modern reachability analysis approaches for parametric ordinary differential-algebraic equations (Villanueva et al., 2015).

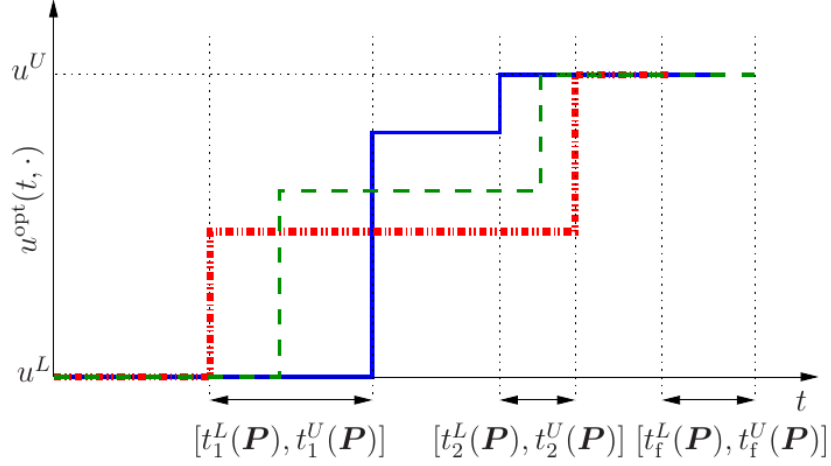


Figure 2: Illustration of the parameterization of the optimal control policy under uncertainty with nominal policy (green dashed line) and extreme-case realizations (dash-dotted red and solid blue lines).

4.2. Robust approach to real-time optimization

The result (15), in practice, establishes a parametric solution to the real-time optimization problem. Its implementation can be performed in a robust fashion to determine the parameters of the optimal-control structure that lead to the best performance in the worst case. We can then solve

$$\min_{\substack{u_s(t, \mathbf{p}) \in U^{\text{opt}}(t), \forall t \in [t_1(\mathbf{p}), t_2(\mathbf{p})] \\ t_i \in T_i, \forall i \in \{1, 2, f\}}} \max_{\mathbf{p} \in \mathbf{P}_0} \|\mathcal{J}(\mathbf{p}) - \mathcal{J}(\mathbf{p}_0^{\text{nom}})\|_2^2 \quad \text{s.t. (1b), (9), (10), (17)}$$

for a given $\mathbf{x}(0) = \mathbf{x}_0$ and \mathbf{P}_0 . Here we propose to minimize the variance of the objective w.r.t. nominal scenario under the worst-case realization of $\mathbf{p} \in \mathbf{P}$, which can also be modified to $\|\mathcal{J}(\mathbf{p}) - \min_{\mathbf{p}^{\text{opt}} \in \mathbf{P}_0} \mathcal{J}(\mathbf{p}^{\text{opt}})\|_2^2$. Note that this goal goes in line with the efforts of practical batch process control, where the reduction of the batch-to-batch variability is one of the main targets of decision making.

4.3. Robust adaptive approach to real-time optimization

In order to reduce conservatism of a robust scheme, parameter estimation can be used for exploitation of data gathered along the process run. The employed parameter estimation scheme should take into account the presence of noise in the measurements. Here we propose to use set-membership strategy outlined in Section 3.2.

The problem (17) can then be resolved with the initial state conditions $\mathbf{x}(k) = \mathbf{x}_k$ and with updated parameter bounds \mathbf{P}_k in a shrinking-horizon fashion. Computational efficiency of this real-time optimization scheme can be achieved by exploiting the fact that the re-optimization does not need to be done at each sampling time of the plant (i.e., when new measurements become available) but can be scheduled before a consecutive switching event must be realized. As an example, consider Fig. 2, where one can start the operation on the lower-bound of the input variable and estimation of parameter bounds and re-optimization can be scheduled in the sampling instant of the plant just before minimal value of the time $t_1, t_1^L(\mathbf{P})$. The re-optimization with updated bounds on parameters would then update (possibly increase) the value of $t_1^L(\mathbf{P})$. Further re-optimizations can then follow based on this scheme.

Once the optimal value of the objective function of (17) reaches $\|\mathcal{J}(\mathbf{P}) - \mathcal{J}(\mathbf{p}_k^{\text{nom}})\|_2^2 < \varepsilon$, where $\varepsilon > 0$ represents user-defined tolerance for the worst-case cost variation, the calculated control actions can be implemented until the end of the batch, e.g., with a feedback scheme (François and Bonvin, 2013), until the terminal conditions are met.

Note that because of the switching nature of the optimal control strategy, the proposed problem might show discontinuity when the set of active

constraints changes. This can be remedied by the adaptation of continuous-formulation technique presented in de Prada et al. (2011).

A pseudo-algorithm can be devised at this point to summarize the proposed approach:

1. Given the problem setup (Eqs. (1) and (2)), identify the solution structure using Pontryagin’s minimum principle (as shown in Section 3.1).
2. Given \mathbf{P}_0 , use reachability analysis to project the uncertainty in the parameters to uncertainty about the solution structure (as shown in Section 4.1).
3. Apply the optimal policy until the next uncertain switching time and collect the measurements along.
4. Solve problem (14) to determine new interval box \mathbf{P} and re-calculate the uncertain solution structure.
5. If significant reduction in the uncertainty of the switching time is achieved, go to Step 3. Else solve problem (17) to determine the switching times. Apply the first switching in the control, collect the data along and go to Step 4.

5. Case study

We demonstrate the findings of this study on an example of time-optimal control of a batch diafiltration process (Cheryan, 1998). This is a membrane-based separation process designed for a simultaneous concentration of valuable products in the liquid solutions (referred to as macro-solutes) and a wash-out of the impurities (referred to as micro-solute).

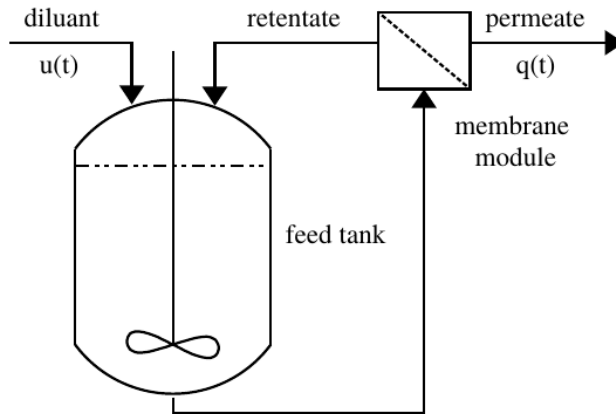


Figure 3: Schematic representation of a generalized diafiltration process.

A simplified scheme of the plant is shown in Fig. 3. After the separated solution with initial volume (V_0) comprising a macro-solute (high molecular weight component) and a micro-solute (low molecular weight component) with initial concentrations $c_{1,0}$ and $c_{2,0}$, respectively, is transferred to the feed tank, the operation of the process is launched. Solution containing diluant (solvent), micro-solute and macro-solute is taken from the feed tank to the membrane module. The installed membrane is designed in a way to allow passage of micro-solute and to retain macro-solute. Permeate stream then leaves the system with the flow rate q which is specific for a given membrane, operating conditions and is often a function of actual concentrations of separated species. Retentate stream is then introduced back into the feed tank. Once the final conditions, which are the prescribed final concentrations of the species $c_{1,f}$ and $c_{2,f}$, are met, the process is terminated and the solution is withdrawn from the system. During the operation, the transmembrane pressure is controlled at a constant value. The temperature of the solution is maintained around a constant value using a heat exchanger (not shown in

Fig. 3 for the sake of simplicity). The manipulated variable $u(t)$ is the ratio between fresh water inflow into the tank and the permeate outflow q .

In our study, the outflow q is measured at intervals of one minute and its model is given by

$$\begin{aligned}
 q(\underbrace{c_1(t), c_2(t)}_{\mathbf{c}(t)}, \underbrace{\gamma_1, \gamma_2, \gamma_3}_{\boldsymbol{\gamma}}) &= A\gamma_1 \ln\left(\frac{\gamma_2}{c_1(t)c_2^{\gamma_3}(t)}\right) \\
 &= A\gamma_1 [\ln(\gamma_2) - \ln(c_1(t)) - \gamma_3 \ln(c_2(t))], \\
 q(\mathbf{c}(t), \underbrace{p_1, p_2, p_3}_{\mathbf{p}}) &= p_1 - p_2 \ln(c_1(t)) - p_3 \ln(c_2(t)). \tag{18}
 \end{aligned}$$

Here the parameters γ_1 , γ_2 , and γ_3 can be related to phenomenological constants; γ_1 stands for the mass-transfer coefficient, γ_2 is the limiting concentration of the macro-solute, and γ_3 is a dimensionless non-ideality factor. This model is proposed in Rajagopalan and Cheryan (1991) as a generalization of a limiting-flux model, which originates from film-theory of mass transfer (Fick, 1855) and where $\gamma_3 = 0$. We study situations where the permeate flux at the plant obeys either one of these models.

As Eq. (18) suggests, an equivalent re-parameterization of the model is possible, which gives the model linear in parameters p_1 , p_2 , and p_3 . This is convenient for parameter estimation. In this work, we will assume that the concentrations $c_1(t)$ and $c_2(t)$ can be measured perfectly (i.e., their measurement sensors are noise-free). As the values of state variables are known exactly, the dynamic equations can be eliminated from the problem (14). Hence, the problem of estimating bounds of the model parameters (14) boils down to a problem of linear programming, since dynamics can be excluded and since the re-parameterization of the model yields linear-in-parameters

structure of the model. The measurement noise associated with q is assumed to be bounded $\sigma = 0.1L/h$ and the measurements are available each second. In the simulation studies below, the realization of noise will be taken from a uniform distribution $\mathcal{U}(-\sigma, \sigma)$.

The objective is to find $u(t)$, which guarantees the transition from the given initial ($c_{1,0}$ and $c_{2,0}$) to final ($c_{1,f}$ and $c_{2,f}$) concentrations in minimum time. This problem can be formulated as:

$$\min_{t_f, u(t)} \int_0^{t_f} 1 dt, \quad (19a)$$

$$\text{s.t.} \quad \dot{c}_1(t) = \frac{c_1^2(t)q(\mathbf{c}(t), \mathbf{p})}{c_{1,0}V_0}(1 - u(t)), \quad c_1(0) = c_{1,0}, \quad c_1(t_f) = c_{1,f}, \quad (19b)$$

$$\dot{c}_2(t) = -\frac{c_1(t)c_2(t)q(\mathbf{c}(t), \mathbf{p})}{c_{1,0}V_0}u(t), \quad c_2(0) = c_{2,0}, \quad c_2(t_f) = c_{2,f}, \quad (19c)$$

$$q(\mathbf{c}(t), \mathbf{p}) = p_1 - p_2 \ln(c_1(t)) - p_3 \ln(c_2(t)), \quad (19d)$$

$$u(t) \in [0, \infty). \quad (19e)$$

The parameters of the problem are $c_{1,0} = 50$ g/L, $c_{1,f} = 150$ g/L, $c_{2,0} = 50$ g/L, $c_{2,f} = 0.05$ g/L, $V_0 = 20$ L, and $A = 1$ m². Note that the extremal values of $u(t)$ in (19e) stand for a mode with no water addition, when $u(t) = 0$ and pure dilution, i.e., a certain amount of water is added at a single time instant, $u(t) = \infty$.

The parameterized optimal control of this process can be identified using Pontryagin's minimum principle (Pontryagin et al., 1962) as (9) where the singular control and the respective switching function can be found explic-

itly (Paulen et al., 2012) as

$$u_s(\mathbf{c}(t, \mathbf{p}), \mathbf{p}) := \frac{1}{1 + \gamma_3} = \frac{p_2}{p_2 + p_3}, \quad (20)$$

$$\begin{aligned} S(\mathbf{c}(t, \mathbf{p}), \mathbf{p}) &:= A\gamma_1 (\ln(\gamma_2) - \ln(c_1) - \gamma_3 \ln(c_2) - \gamma_3 - 1), \\ &:= \underbrace{p_1 - p_2 \ln(c_1) - p_3 \ln(c_2)}_{q(\mathbf{c}(t), \mathbf{p})} - p_2 - p_3. \end{aligned} \quad (21)$$

The structure of the optimal-control policy clearly reveals that the singular arc condition gives a constant value for the permeate flux (equal to $p_2 + p_3$) and that the singular control is a constant that depends on the value of $\gamma_3 = p_3/p_2$. This shows that if one devises a feedback-based real-time optimization scheme, precise estimation of parameters p_2 and p_3 is of paramount interest.

For the simulation-based studies on the implementation of the outlined optimal-control policy, we will assume that the nominal values of the parameters are $\gamma_1 = 3 \times 10^{-2}$ L/h, $\gamma_2 = 1000$ g/L, and $\gamma_3 = 0.1$. Similar values of the parameters were observed to validate the model against experimental data in Sharma et al. (2019). The uncertainty at the initial point in time (\mathbf{P}_0) will be assumed as $\pm 10\%$ of the nominal values. The true realization of the parameter values will be taken randomly from a uniform distribution $\mathcal{U}(p_0^L, p_0^U)$. As we deal with a time-minimization problem and the sampling time of the plant is 1 second, we naturally select the $\varepsilon = 1$ s². For this simple example, the reachability analysis can be performed explicitly using the expressions for switching times provided in Paulen and Fikar (2016).

5.1. Plant under limiting-flux conditions

We first study the case when the plant is under limiting-flux conditions, i.e., the flux obeys Eq. (18) with $\gamma_3 = p_3 = 0$. Based on the values of initial

conditions and range of uncertainty in the parameters, the optimal-control policy boils down to three arcs:

1. Use $u(t) = 0$ until t_1 , when $c_1(t_1) = \gamma_2/e$.
2. Use $u(t) = u_s(t) = 1$ until $c_1(t_2)/c_2(t_2) = c_{1,f}/c_{2,f}$.
3. Dilute the solution (use $u(t) = \infty$ instantaneously) to arrive at the final concentrations.

Taking into account that we measure both concentrations precisely, the only uncertainty in this case lies in the switching times t_1 , where t_1 depends on the value of γ_2 .

The implementation of the scheme, where one is aware of the true value of γ_2 , results in $t_1^{\text{opt}} = 2.515$ h and $t_f^{\text{opt}} = 8.284$ h. The worst-case minimization of the batch variability (methodology described in Section 4.2) coincides in this case with the nominal strategy, where one takes $\gamma_2 = \gamma_2^{\text{nom}}$. When applied to the plant, this strategy results in $t_1^{\text{rob}} = t_1^{\text{nom}} = 2.625$ h and $t_f^{\text{rob}} = t_f^{\text{nom}} = 8.327$ h. The adaptive real-time dynamic optimization (described in Section 4.3) results in $t_1^{\text{adapt}} = 2.533$ h and $t_f^{\text{adapt}} = 8.301$ h, which is only a slight improvement compared to the robust (and nominal) strategy.

Figure 4 presents performance of the estimation (in terms of estimated parameter bounds) throughout the run of the batch. It is clear that the bounds on both parameters are dramatically reduced around the time point of 2 h, which precedes the time point t_1^{opt} , when the switch in the control input should be executed. The bottom plot of Fig. 4 also shows the evolution of the uncertainty in t_1 , which is projected using interval-based calculations (as discussed in Section 4.1). It should be noted here that the adaptive approach is successful mainly since the applied control input in the first arc coincides

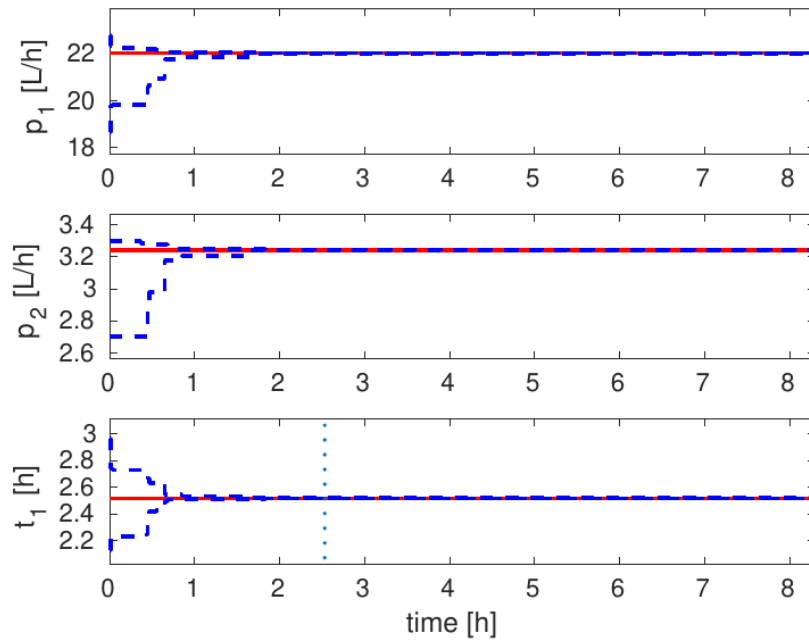


Figure 4: Results of the set-membership estimation over time (top and middle plots) with projection of the uncertainty in the parameters on the switching time t_1 (bottom plot). The true (optimal) values are shown as solid lines, the bounds are represented using dashed lines. The vertical line in the bottom plot indicates the optimal switching time.

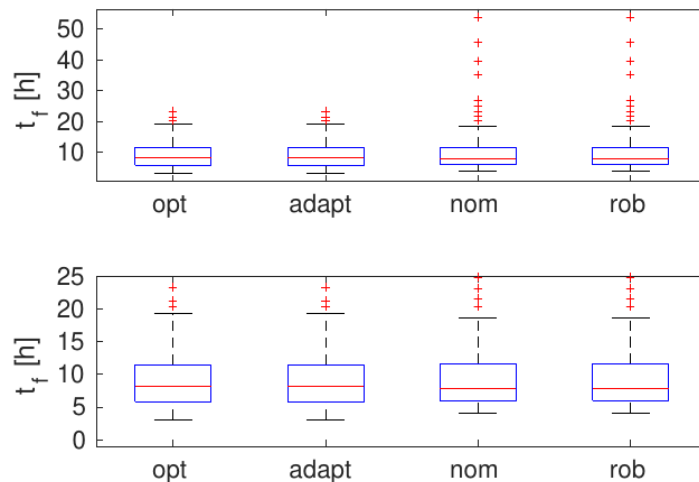


Figure 5: A box plot with the statistical information (the median, the 25th and 75th percentiles and the outliers) about the performance of the different control strategies on the plant under limiting-flux conditions. The bottom plot shows a zoom of the top plot.

with an input that would result from a dynamic optimal-experiment design study. Here, $u(t) = 0$ ensures the fastest possible increase of concentration $c_1(t)$, which reveals the most informative measurements about γ_2 .

Finally, we evaluate a statistical performance of the presented dynamic real-time optimization schemes. This is realized by running 1,000 simulated batches with different true values of parameters. The resulting statistics is shown in Fig. 5. One can clearly notice here that the robust and nominal strategies perform very well on average and even the standard deviations of their performance are not significantly increased compared to the optimal performance. On the other hand, distributions of the final batch times of the nominal and robust strategies have long tails, which points towards the existence of rare cases where the batch time obtained by application of robust dynamic real-time optimization increases significantly compared to the truly

optimal solution. This behavior corresponds to the situations, where the first step (with $u(t) = 0$) over-concentrates the solution too much so that the subsequent diafiltration step (with $u(t) = 1$) requires long time to reach the desired condition ($c_1(t_2)/c_2(t_2) = c_{1,f}/c_{2,f}$). This study reveals that the strategy, which uses estimation of parameter bounds, has a clear merit as it does not show this type of inconsistency in the performance (long tails) and it results overall in the batch times very close to the optimal ones.

Drawing a comparison in the computational time, robust and nominal strategies only require a single optimization before the batch starts. Adaptive strategy uses only a single re-optimization (scheduled just before t_1^{nom}) in this case, which shows a significant reduction in computational burden w.r.t. receding-horizon strategies. Due to explicit nature of the optimal control strategy, the computation of this re-optimization mostly lies in the estimation step. As the estimation problem can be boiled down to an LP, its solution is available in order of milliseconds using MATLAB's *linprog* routine. Due to only a single re-optimization, one can also interpret this scheme as a mid-course correction (Yabuki et al., 2002) with optimally timed adaptation.

5.2. Plant under generalized limiting-flux conditions

Based on the values of initial conditions and range of uncertainty in the parameters, the optimal-control policy again boils down to three arcs:

1. Use $u(t) = 0$ until t_1 , when (21) is zero.
2. Use $u(t) = u_s(t) = 1/(1 + \gamma_3)$ until $c_1(t_2)/c_2(t_2) = c_{1,f}/c_{2,f}$.
3. Dilute the solution (use $u(t) = \infty$ instantaneously) to arrive at the final concentrations.

The uncertainty is in this case extended even on the value of singular control input and it is clear that one needs good estimates of both the values of γ_2 (which mostly influences the switching time t_1 as in the previous case) and γ_3 (which influences the quality of the singular control) to achieve a good performance. Knowledge of the a precise value of the parameter γ_1 is of minor importance as this parameter can be factored out of the optimality conditions.

We use the same values of the uncertain parameters γ_1 and γ_2 as in the previous case. The performance of the studied schemes is as follows:

- Optimal strategy: $t_1^{\text{opt}} = 2.501$ h, $t_f^{\text{opt}} = 9.254$ h
- Adaptive strategy: $t_1^{\text{adapt}} = 2.510$ h and $t_f^{\text{adapt}} = 9.271$ h
- Nominal strategy: $t_1^{\text{nom}} = 2.561$ h and $t_f^{\text{nom}} = 9.277$ h
- Robust strategy: $t_1^{\text{rob}} = 2.417$ h and $t_f^{\text{rob}} = 9.269$ h

We can observe a similar differences between the strategies as in the previous case. Robust strategy performs on an acceptable level and even marginally outperforms the nominal and the adaptive strategy, which results from the fact that the plant parameters coincide with the worst-case parameters.

Figure 6 presents performance of the estimation (in terms of estimated parameter bounds) throughout the run of the batch. Similarly to the previous case, the estimation performed in the first control arc helps in determination of the value of the first switching time before the optimal switching instant occurs. Here the determining parameter is p_2 , whose estimation performance was discussed in the previous case and the same conclusions hold here.

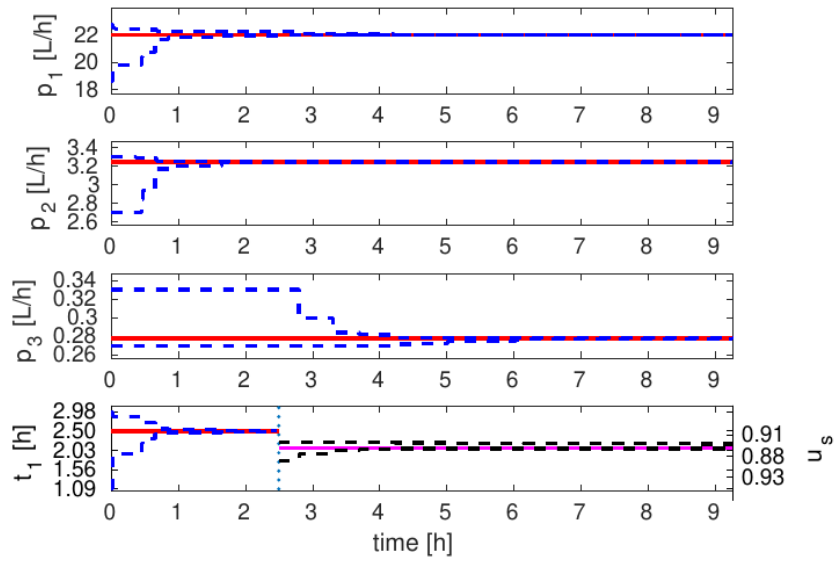


Figure 6: Results of the set-membership estimation over time (top three plots) with projection of the uncertainty in the parameters on the switching time t_1 and on the value of u_s (bottom plot). The true (optimal) values are shown as solid lines, the bounds are represented using dashed lines. The vertical line in the bottom plot indicates the optimal switching time.

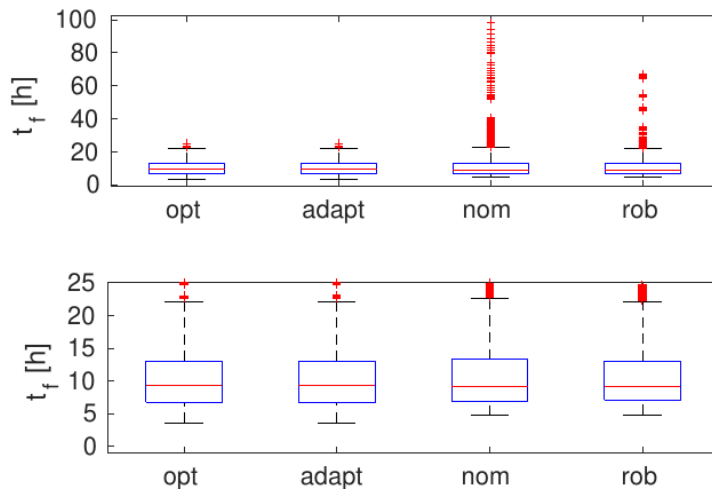


Figure 7: A box plot with the statistical information (the median, the 25th and 75th percentiles and the outliers) about the performance of the different control strategies under generalized limiting-flux conditions. The bottom plot shows a zoom of the top plot.

When the controller applies $u(t) = 0$, the parameter γ_3 (or p_3) is unidentifiable as the concentration $c_2(t)$ remains constant. This can be seen in Fig. 6 as the bounds on p_3 remain constant from the beginning of the operation until the time when control input is switched to singular. It is also shown that the uncertainty in p_3 results in a relatively small uncertainty in the value of the singular control, so a precise knowledge of p_3 is not paramount for the application of the optimal control policy.

When the statistical performance is evaluated, we can first conclude that all the strategies perform almost identically on average. The biggest differences arise when one evaluates the outliers of the distribution of the achieved batch times. It is evident that the nominal strategy achieves the worst performance and that the robust strategy reduces the batch variability to a good extent (given the wide range of the uncertainty). The adaptive strat-

egy is clearly superior here as it reduces the batch variability much further, compared to the robust scheme, and the achieved performance is practically indistinguishable from the truly optimal one.

6. Conclusion

We have presented a methodology for dynamic real-time optimization of batch processes via parameterization of the optimal controller using Pontryagin's minimum principle. The employed parameterization greatly reduces the computational burden to guarantee feasibility of the operation compared to receding-horizon strategies. In order to address parametric plant-model mismatch issue, we have suggested a robust approach, which consisted in projection of the plant uncertainty into optimality conditions using reachability analysis. This again greatly reduces on-line computational burden as one can exploit the uncertainty in the switching to schedule the on-line re-optimization. As the uncertainty in parameters can greatly affect the optimality of the batch, we have proposed an adaptive scheme that makes use of parameter estimation and, as shown in the case study, can greatly assist in reducing variability in the batch performance subject to parametric uncertainty. The adaptive scheme turned out to be key in reduction of batch-to-batch variability. The future work will consider implementation of the proposed strategy on a laboratory plant.

Acknowledgments

The authors gratefully acknowledge the contribution of the Scientific Grant Agency of the Slovak Republic under the grant 1/0004/17, of the Slo-

vak Research and Development Agency under the project APVV 15-0007 and of the European Commission under the grant 790017 (GuEst). This publication is also a partial result of the Research & Development Operational Programme for the project University Scientific Park STU in Bratislava, ITMS 26240220084, supported by the Research 7 Development Operational Programme funded by the ERDF. This work was also supported by the funding from Slovak Ministry of Education, Science, Research and Sport under the project STU as the Leader of Digital Coalition 002STU-2-1/2018.

Notation

t	time [h]
\boldsymbol{x}	vector of state variables
\boldsymbol{p}	vector of model parameters
u	manipulated variable
\mathcal{J}	objective functional
F_0	constant-in-control part of the Lagrange term
F_u	multiplier of linear-in-control part of the Lagrange term
\boldsymbol{f}_0	constant-in-control term of the model
\boldsymbol{f}_u	multiplier of linear-in-control term of the model
\boldsymbol{P}	interval box
H	Hamiltonian (function)
H_0	constant-in-control term of the Hamiltonian
H_u	multiplier of linear-in-control term of the Hamiltonian
μ	Lagrange multiplier of bound on manipulated variable
ν	Lagrange multiplier of final conditions

$\lambda(\cdot)$	vector of adjoint variables
S	state-dependent switching function
π	vector parameterizing the optimal control strategy
g	measurement function
y	vector of predicted plant outputs
$y_p(t)$	vector of true outputs of the plant
$y_m(t)$	vector of measured outputs
σ	magnitude of measurement noise
mid	mid-point of the interval box
ε	user-defined tolerance
A	membrane area [m ²]
V	volume of the processed solution
c_1	macro-solute concentration
c_2	micro-solute concentration
q	permeate flux, flow rate through the membrane
γ_1	mass-transfer coefficient
γ_2	limiting concentration of the macro-solute
γ_3	dimensionless non-ideality factor
γ	parameters of the original permeate-flux model
p_1, p_2, p_3	parameters of the reparametrized permeate-flux model
$\mathcal{U}(a, b)$	uniform distribution bounded by a and b
<i>Subscripts</i>	
0	initial, control-independent
u	linear-in-control part
k	sampling instant of the plant

f final
s singular

Superscripts

L lower bound
 U upper bound
opt optimal
nom nominal
adapt adaptive
rob robust

References

- Adetola, V., DeHaan, D., Guay, M., 2009. Adaptive model predictive control for constrained nonlinear systems. *Systems & Control Letters* 58 (5), 320 – 326.
- Amrhein, M., Bhatt, N., Srinivasan, B., Bonvin, D., 11 2010. Extents of reaction and flow for homogeneous reaction systems with inlet and outlet streams. *AIChE Journal* 56.
- Aydin, E., Bonvin, D., Sundmacher, K., 2018. Toward fast dynamic optimization: An indirect algorithm that uses parsimonious input parameterization. *Industrial & Engineering Chemistry Research* 57 (30), 10038–10048.
- Cao, Y., Li, S., Petzold, L., Serban, R., 2003. Adjoint sensitivity analysis for differential-algebraic equations: The adjoint dae system and its numerical solution. *SIAM Journal on Scientific Computing* 24 (3), 1076–1089.

- Chachuat, B., Houska, B., Paulen, R., Perić, N. D., Rajyaguru, J., Villanueva, M. E., 2015. Set-theoretic approaches in analysis, estimation and control of nonlinear systems. *IFAC-PapersOnLine* 48 (8), 981–995.
- Cheryan, M., 1998. *Ultrafiltration and microfiltration handbook*. CRC press, Florida, USA.
- de Prada, C., Rodriguez, M., Sarabia, D., 2011. On-line scheduling and control of a mixed continuous-batch plant. *Industrial & Engineering Chemistry Research* 50 (9), 5041–5049.
- Fick, A., 1855. Ueber diffusion. *Annalen der Physik* 170 (1), 59–86.
- Fogel, E., Huang, Y., 1982. On the value of information in system identification – bounded noise case. *Automatica* 18 (2), 229 – 238.
- François, G., Bonvin, D., 2013. Chapter one - measurement-based real-time optimization of chemical processes. In: Pushpavanam, S. (Ed.), *Control and Optimisation of Process Systems*. Vol. 43 of *Advances in Chemical Engineering*. Academic Press, pp. 1 – 50.
- François, G., Srinivasan, B., Bonvin, D., 2005. Use of measurements for enforcing the necessary conditions of optimality in the presence of constraints and uncertainty. *Journal of Process Control* 15 (6), 701 – 712.
- Gottu Mukkula, A. R., Paulen, R., 2017. Model-based design of optimal experiments for nonlinear systems in the context of guaranteed parameter estimation. *Computers & Chemical Engineering* 99, 198 – 213.

- Hangos, K. M., Bokor, J., Szederkényi, G., 2006. Analysis and control of nonlinear process systems. Springer.
- Hosseini, A., Oshaghi, M., Engell, S., 2013. Control of particle size distribution in emulsion polymerization using mid-course correction under structural plant-model mismatch*. IFAC Proceedings Volumes 46 (32), 529 – 534, 10th IFAC International Symposium on Dynamics and Control of Process Systems.
- Jang, H., Lee, J. H., Biegler, L. T., 2016. A robust nmPC scheme for semi-batch polymerization reactors. IFAC-PapersOnLine 49 (7), 37 – 42, 11th IFAC Symposium on Dynamics and Control of Process Systems Including Biosystems DYCOPS-CAB 2016.
- Jaulin, L., Walter, E., 1993. Set inversion via interval analysis for nonlinear bounded-error estimation. Automatica 29 (4), 1053–1064.
- Johnson, C. D., Gibson, J. E., 1963. Singular solutions in problems of optimal control 8 (1), 4–15.
- Liou, C., Hsiue, T., 1995. Exact linearization and control of a continuous stirred tank reactor. Journal of the Chinese Institute of Engineers 18 (6), 825–833.
- Lucia, S., Finkler, T., Engell, S., 2013. Multi-stage nonlinear model predictive control applied to a semi-batch polymerization reactor under uncertainty. J Process Contr 23 (9), 1306 – 1319.
- Martí, R., Lucia, S., Sarabia, D., Paulen, R., Engell, S., de Prada, C., 2015.

- Improving scenario decomposition algorithms for robust nonlinear model predictive control. *Computers & Chemical Engineering* 79, 30–45.
- Nagy, Z. K., Braatz, R. D., 2003. Robust nonlinear model predictive control of batch processes. *AIChE Journal* 49 (7), 1776–1786.
- Paulen, R., Fikar, M., 2016. *Optimal Operation of Batch Membrane Processes*. Springer.
- Paulen, R., Fikar, M., Foley, G., Kovács, Z., Czermak, P., 2012. Optimal feeding strategy of diafiltration buffer in batch membrane processes. *Journal of Membrane Science* 411-412, 160–172.
- Paulen, R., Jelemenský, M., Kovács, Z., Fikar, M., 2015. Economically optimal batch diafiltration via analytical multi-objective optimal control. *Journal of Process Control* 28, 73 – 82.
- Paulen, R., Villanueva, M. E., Chachuat, B., 2016. Guaranteed parameter estimation of non-linear dynamic systems using high-order bounding techniques with domain and cpu-time reduction strategies. *IMA Journal of Mathematical Control and Information* 33 (3), 563–587.
- Pontryagin, L. S., Boltyanskii, V. G., Gamkrelidze, R. V., Mishchenko, E. F., 1962. *The Mathematical Theory of Optimal Processes*. John Wiley & Sons, Inc., New York.
- Rajagopalan, N., Cheryan, M., 1991. Process Optimization in Ultrafiltration: Flux-Time Considerations in the Purification of Macromolecules 106 (1), 57–69.

- Rodrigues, D., Bonvin, D., 2019. Dynamic optimization of reaction systems via exact parsimonious input parameterization. *Industrial & Engineering Chemistry Research*In Press.
- Schlegel, M., Marquardt, W., 2006. Detection and exploitation of the control switching structure in the solution of dynamic optimization problems. *Journal of Process Control* 16 (3), 275 – 290, selected Papers from Dycops 7 (2004), Cambridge, Massachusetts Seventh {IFAC} Symposium on the Dynamics and Control of Process Systems (Dycops-7).
- Schlegel, M., Stockmann, K., Binder, T., Marquardt, W., 2005. Dynamic optimization using adaptive control vector parameterization. *Computers & Chemical Engineering* 29 (8), 1731 – 1751.
- Schweppe, F., 1968. Recursive state estimation: Unknown but bounded errors and system inputs. *IEEE Transactions on Automatic Control* 13 (1), 22–28.
- Sharma, A., Valo, R., KalÁžz, M., Paulen, R., Fikar, M., 2019. Implementation of optimal strategy to economically improve batch membrane separation. *Journal of Process Control* 76, 155 – 164.
- Sontag, E. D., 1998. *Mathematical Control Theory: Deterministic Finite Dimensional Systems* (2nd Ed.). Springer-Verlag, Berlin, Heidelberg.
- Srinivasan, B., Bonvin, D., Visser, E., Palanki, S., 2003a. Dynamic optimization of batch processes: Ii. role of measurements in handling uncertainty. *Computers & Chemical Engineering* 27 (1), 27 – 44.
- Srinivasan, B., Palanki, S., Bonvin, D., 2003b. Dynamic optimization of batch

- processes: I. Characterization of the nominal solution. *Computers & Chemical Engineering* 27 (1), 1–26.
- Villanueva, M. E., Houska, B., Chachuat, B., 2015. Unified framework for the propagation of continuous-time enclosures for parametric nonlinear odes. *Journal of Global Optimization* 62 (3), 575–613.
- Walz, O., Djelassi, H., Caspari, A., Mitsos, A., 2018. Bounded-error optimal experimental design via global solution of constrained $\min\text{-}\max$ program. *Computers & Chemical Engineering* 111, 92 – 101.
- Yabuki, Y., MacGregor, J. F., 1997. Product quality control in semibatch reactors using midcourse correction policies. *Industrial & Engineering Chemistry Research* 36 (4), 1268–1275.
- Yabuki, Y., Nagasawa, T., MacGregor, J. F., 2002. Industrial experiences with product quality control in semi-batch processes. *Computers & Chemical Engineering* 26 (2), 205 – 212.